

Electronic Supplementary Information

Highly efficient formic acid and carbon dioxide electro-reduction to alcohols on indium oxide electrodes

Kayode Adesina Adegoke,¹ Shankara Gayathri Radhakrishnan,¹ Clarissa L. Gray,¹ Barbara Sowa,¹ Claudia Morais,² Paul Rayess,² Egmont, R. Rohwer, Clément Comminges,² K. Boniface Kokoh,² Emil Roduner^{1,3*}

¹ Department of Chemistry, University of Pretoria, Pretoria 0002, South Africa

² Université de Poitiers, 4 rue Michel Brunet, IC2MP UMR-CNRS 7285, TSA 51106, 86073 Poitiers cedex 9, France

³ Institute of Physical Chemistry, University of Stuttgart, Pfaffenwaldring 55, D-70569 Stuttgart, Germany

Methods

Materials and reagents

The following analytical grade chemicals were used without further treatment: hexachloroiridic acid ($\text{H}_2\text{IrCl}_6 \cdot 4\text{H}_2\text{O}$, Alfa Aesar, 99%, Ir 38-42%), tantalum carbide (TaC, Aldrich, $\geq 5 \mu\text{m}$, 99%), iso-propanol (Sigma-Aldrich, HPLC 99.9%), methanol, ethanol (Sigma-Aldrich, HPLC 99.9%), NaNO_3 (Sigma-Aldrich, $\geq 99\%$), $\text{In}(\text{NO}_3)_3 \cdot 9\text{H}_2\text{O}$ (Sigma-Aldrich, 99.99% metal basis), NH_4OH (Sigma-Aldrich, 28.0-30.0% NH_3), Na_2SO_4 (Riedel-de Haën, 99%), Nafion® perfluorinated resin solution (Sigma-Aldrich, 5 wt% in lower aliphatic alcohols and water), polytetrafluoroethylene (Sigma-Aldrich, 60 wt% dispersion in water), H_2O_2 (Alfa Aesar, 35% w/w aq. stabilized solution), H_2SO_4 (Sigma-Aldrich, 95-97%), formic acid (Radchem Pty. Ltd, 99%). Deionised water of 18.2 M Ω .cm resistivity was produced by a Millipore® water purification system which was fed with water ($\approx 10 \text{ M}\Omega$.cm resistivity) produced by Elga Micra Labwater purification system. Materials used were: Nafion® 117 membranes, titanium mesh and carbon paper (Toray-H-060, wet proofed) were obtained from the Fuel Cell Store, USA and used as explained below.

Synthesis of IrO_2 electrocatalyst

The modified Adams' fusion method¹ employed in this study involves the fusion of the metal chloride precursor with NaNO_3 by heating to 500 °C at 250 °C /h.² The method has been used to prepare various noble metal oxides.³⁻⁷

Iridic acid was used as the metal precursor and tantalum carbide as the support material. Since iridium is not only expensive but also scarce, the imminent practical application of the process necessitates the reduction of IrO_2 at the anode of PEM water electrolyzers. Among the above literature, TaC has been proven to be suitable as an anode electrocatalyst support since it is stable in the strongly reducing environment that is harsher than in a fuel cell. A predetermined amount of iridic acid was weighed into a crucible, followed by addition of a predetermined amount of TaC which was transferred quantitatively from the glass weighing funnel using 10 mL isopropanol and stirred magnetically for 1 h. Thereafter, NaNO_3 was added in a 17-fold excess over Ir, further stirred for 30 minutes, and heated at 70 °C until a sludge formed. The stirring bar was removed, and the crucible placed in the furnace, heated to 500 °C at 250 °C h^{-1} , left to dwell for 1 h and then allowed to cool to room temperature overnight. The resulting dark grey powder was scraped from the crucible into the centrifuge tube, filled up with 6 mL deionised water and then centrifuged several times, while decanting the supernatant between each run. The resultant powder was washed and filtered to remove the excess NaNO_3 and other water-soluble salts. The paste formed was allowed to dry overnight. In order to limit the sintering of nanosize particles no additional annealing step was introduced.

Synthesis of the In_2O_3 electrocatalyst

2.0 g of $\text{In}(\text{NO}_3)_3 \cdot 9\text{H}_2\text{O}$ was dissolved in 8 mL deionized (DI) water and 23.3 mL ethanol, stirred for 0.5 h at room temperature.^{8,9} 6 mL of NH_4OH was added slowly under stirring until pH = 9 was reached. The slurry formed was aged for 10 min at 80 °C. The white precipitate formed was collected by filtration and then washed with DI water. The resulting precipitate was transferred into a crucible and placed in the furnace to dry for 12 h at 65 °C and then calcined at 300 °C for 3 h to form a yellow solid In_2O_3 .

Preparation of anode and cathode catalysts and gas diffusion layers

For the water splitting reaction a standard TaC-supported IrO_2 water splitting anode catalyst (70:30 wt%, 3.6 mg cm^{-2} loading) was used.¹⁰ The cathode consisted of 7.2 mg cm^{-2} In_2O_3 mixed with Nafion suspension and ethylene glycol binder, coated on carbon paper which was used as gas diffusion layer. For preparation of the gas diffusion electrodes, the carbon paper was first immersed in acetone and sonicated to remove any impurities on the surface. The cleaned paper was rinsed with deionized water and dried in the oven at 90 °C for 1 h. The ink for the cathode electrocatalysts was prepared using the method reported by Sun et al.¹¹ A carefully weighed amount of electrocatalytic powder and a predetermined amount of 5 wt%

Nafion® perfluorinated resin suspension were added and stirred for 1 h. An additional amount of iso-propanol was added, stirred for 15 min and sonicated for 1 h. The resulting ink was left under continuous stirring to ensure a homogeneous suspension. The cathode electrocatalysts were modified by adding either 0.15 wt% or 0.30 wt% of polytetrafluoroethylene (PTFE, 60 wt% dispersion in water) to the In_2O_3 ink to facilitate diffusion. It was then spray-coated in small amounts layer-by-layer onto the carbon paper to avoid clogging, and then dried in hot air at 90 °C before continuing until the desired loading was obtained. The total catalyst loading was 7.5 mg cm^{-2} on a 4 cm^2 geometric active surface area. After completion, the electrocatalyst-loaded carbon paper was finally dried in the oven at 90 °C for 24 h to ensure complete removal of residual water iso-propanol.

Formic acid electrolysis experiments

Electrocatalytic activities of the In_2O_3 and $\text{In}_2\text{O}_3/\text{PTFE}$ catalysts were determined by linear sweep voltammetry (LSV), and the stability was evaluated using chronoamperometry (CA) with a PGStat (Autolab, AUT72638) controlled by Nova® 2.1 software. Experiments were conducted using the cell body of a commercial demonstrator electrolyser cell (H-Tec, Electrolyser Cell 5, Figure 1a) assembled by inserting our homemade membrane electrode assembly consisting of a Nafion® membrane coated with anode electrocatalyst and carbon paper gas diffusion layer coated with cathode electrocatalyst and the current collectors being the titanium mesh. In this two-electrode setup, the voltage is directly the cell voltage. LSV was carried out at room temperature with a scan rate of 10 mV s^{-1} with water and 15% formic acid introduced into the anodic and cathodic chambers, respectively. The liquid products were collected and analysed using our customised Agilent G1530A 6890 gas chromatograph with a split injection port controlled by a two-position actuator module, VICI, Valco instruments Co. Inc., and fitted with flame ionisation detector connected to nickel bed methaniser. The liquid phase column used was a Zebron ZB-Wax column (30 m x 0.25 mm x 0.25 μm) and helium was used as the carrier gas.

Fourier transform infrared (FTIR) spectroscopy coupled with electrochemical experiments

FTIR measurements were carried out using a Bruker IFS 66v spectrometer, which was modified for beam reflection at the electrode surface at a 65° incident angle and fitted with mercury cadmium telluride (MCT/HgCdTe) detector which was cooled with liquid nitrogen. A 10^{-6} bar vacuum was used in order to prevent interferences from atmospheric water and CO_2 . The spectral resolution was 4 cm^{-1} and the FTIR spectra were recorded in the medium infrared range

(MIR) from 1000 to 4000 cm^{-1} on a homemade three-electrode spectroelectrochemical cell (Figure 1b), fitted with a CaF_2 MIR transparent window at the bottom. The working electrode was a 7 mm diameter glassy carbon deposited with In_2O_3 (with or without PTFE). A carbon plate served as a counter electrode, and a saturated calomel (SCE) as the reference electrode, while for convenience and comparability, all potentials were converted to the reversible hydrogen electrode (RHE), following the calculation used by Kim et al.¹² In order to minimize the absorption of the infrared beam by the solution, the working electrode was pressed against the window during measurements so that a thin layer of electrolyte solution was obtained. Single Potential Alteration IR Spectroscopy and Chronoamperometry/FTIR spectroscopy coupling were used. In this method, the electrode reflectivity $R(E_i)$ was recorded subsequently at different potentials E_i , separated by 0.05 V during the potential scan at a sweep rate of 1 mV s^{-1} . In the Chronoamperometry/FTIR method, the potential was maintained at a fixed value and spectra were recorded every 180 s. IR spectra were calculated for each potential value (or time) as changes in the reflectivity (R) relative to a reference single-beam spectrum (R_o) as $R = R_i / R_o$. $R > 1$ and $R < 1$ bands represent the decrease and increase of the concentrations of corresponding species, respectively.

In-situ IR spectro-electrochemical analysis of intermediates

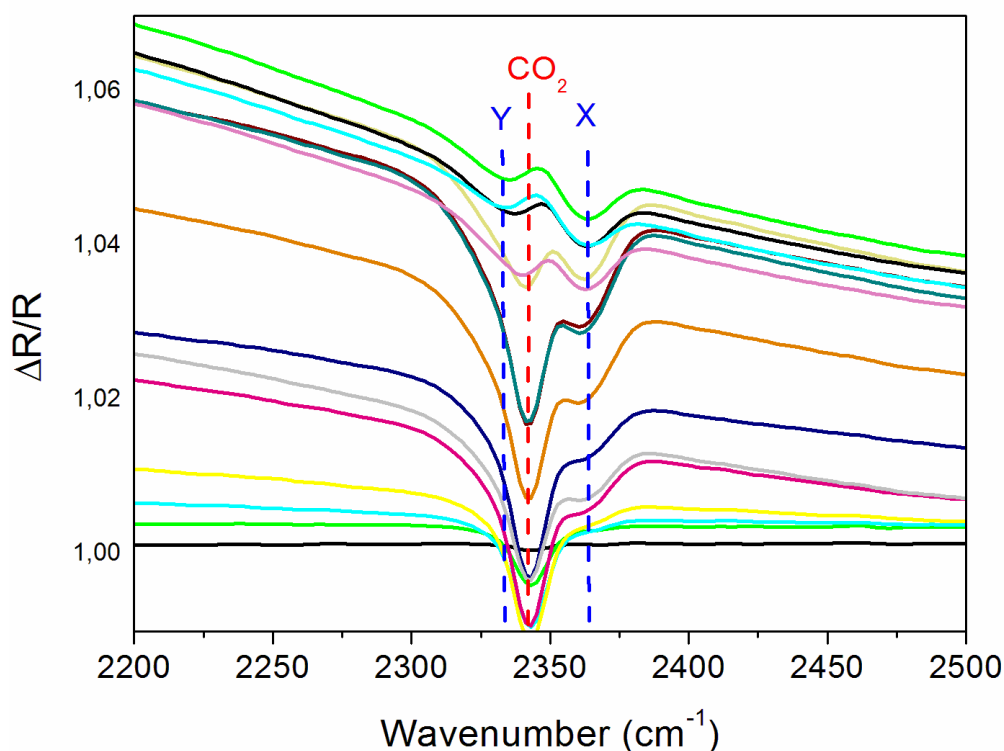


Figure ESI 1: Expanded region around the 2342 cm^{-1} CO_2 band in Figure 3b, showing that CO_2 grows in at oxidative potential (first scan at +1.00 V, interval 100 mV, last scan -0.40 V) and diminishes at

potentials below -0.10 V. A second feature X at 2363 cm^{-1} starts to grow in at $+0.60$ V, and a third small feature Y at 2333 cm^{-1} is seen beyond 0.00 V. This is not the typical doublet of gas phase or dissolved CO_2 , and it is not seen in experiments with progressing time at a constant potential. It is therefore suggested that all three bands represent CO_2 adsorbed on the surface of the catalyst, but at more negative potentials new surface sites become accessible.

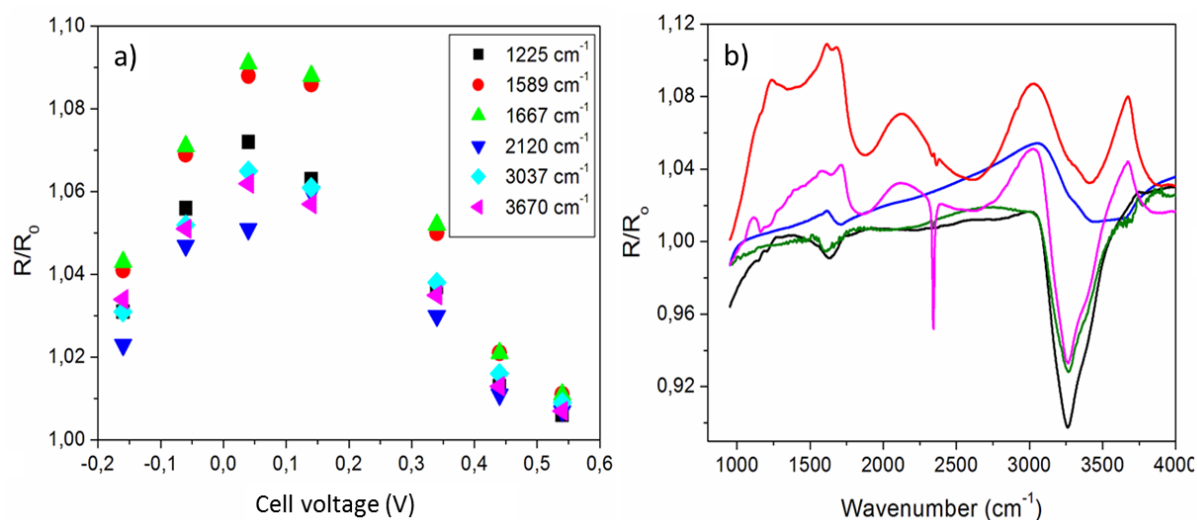


Figure ESI 2: a) Amplitudes of IR bands assigned to FA in Figure 3d as a function of applied potential. The intensities correlate well, suggesting that the bands all belong to the same species. b) IR spectroelectrochemistry of 4.3 M formic acid with PTFE-free In_2O_3 cathode working electrode at a potential of -0.40 V (red, from Figure 3b). IR diffuse reflectance spectra of uncoated glassy carbon electrode without any liquids in the reaction vessel and in the absence of any applied potential. The two broad and asymmetric bands are due to ice that condensed over time on the liquid N_2 -cooled detector (blue). 4.3 M formic acid with 0.30 wt% PTFE-containing In_2O_3 cathode working electrode (magenta). Bare glassy carbon electrode in 0.1 M Na_2SO_4 without any applied voltage (olive). N_2 saturated 0.1 M Na_2SO_4 catholyte with 0.30% PTFE-containing In_2O_3 cathode working electrode (black). The strong band at 3261 cm^{-1} and its weak partner at 1630 cm^{-1} are assigned to the stretching and bending vibrations of $-\text{OH}$ groups bound at the glassy carbon electrode surface.¹³

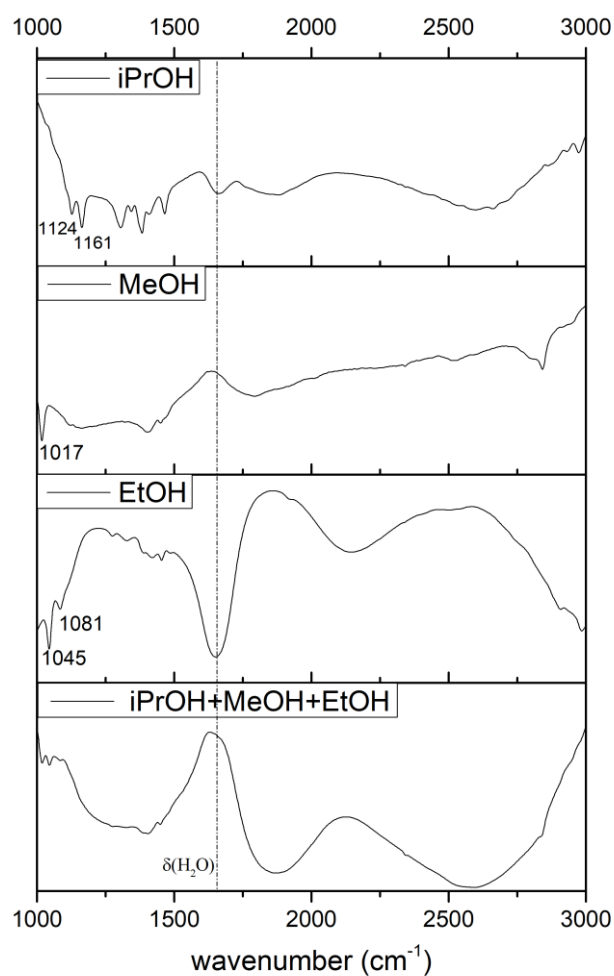


Figure ESI 3: Alcohol (in 0.1 M Na₂SO₄) single scan reflectance reference spectra, indicating the characteristic absorptions in the 1000-1200 cm⁻¹ range and the potential interference of the water bending vibration $\delta(\text{H}_2\text{O})$ near 1600 cm⁻¹.

Table ESI 1: List of IR absorption bands (cm⁻¹) of some pure liquid compounds (source: Aldrich book of IR spectra)

Methanol	1020 (s), 1100 (w), 1430 (m), 2875 (s), 2941 (s), 3330 (s)
Ethanol	881 (s), 1047 (s), 1087 (s), 1390 (m), 2900 (s), 2985 (s), 3330 (s)
Iso-propanol	813 (s), 952 (s), 1124 (s), 1163 (s), 1307 (m), 1370 (s), 1470 (m), 2900 (m), 2985 (s), 3330 (s)
Formic acid	1063 (w), 1190 (s), 1351 (s), 1724 (s), 2564* (m), 2700* (m), 2941 (s), 3125 (s)
Water	1595 (m), 3652 (s), 3756 (s)

strong (s), medium (m), weak (w)

* substructure as a result of splitting due to dimer formation

Calibration of ex-situ GC product analysis

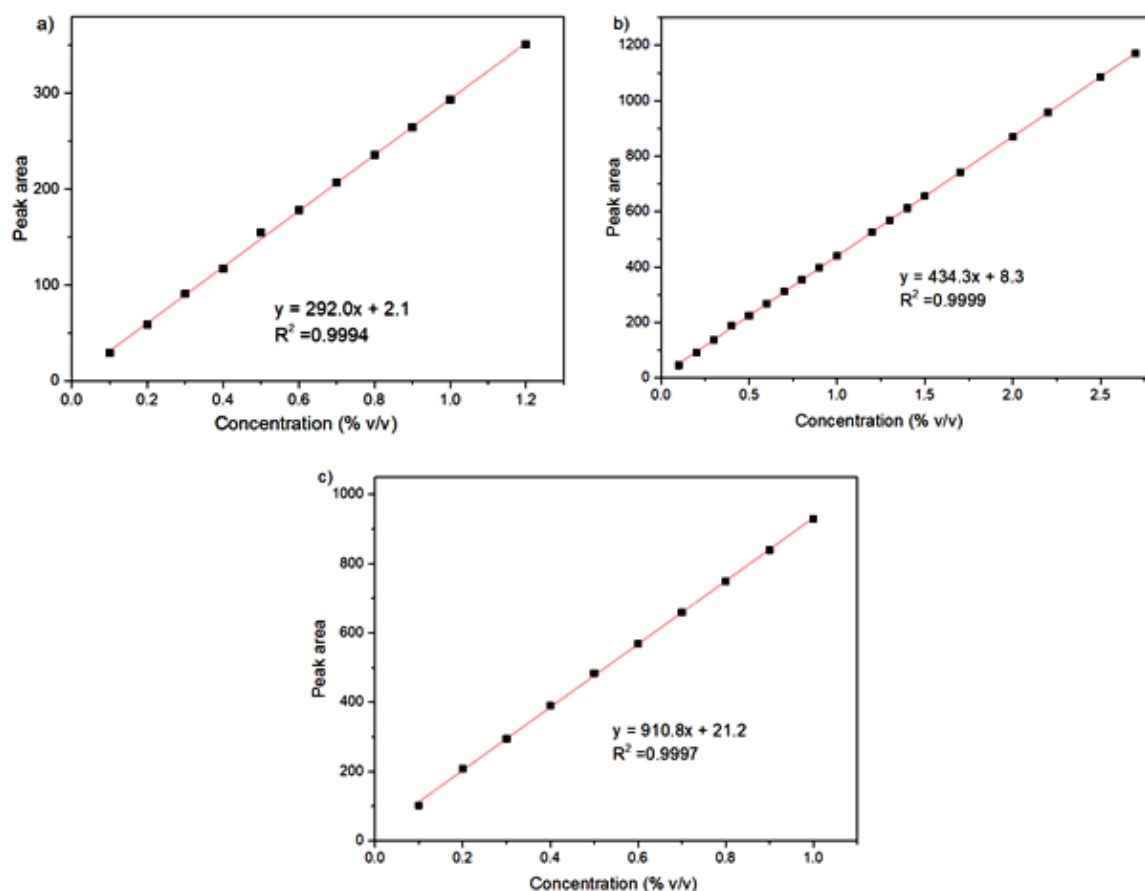


Figure ESI 4: GC calibration curves of (a) methanol, (b) ethanol and (c) iso-propanol, demonstrating good reproducibility with negligible scatter.

Bixbyite structure of crystalline In_2O_3

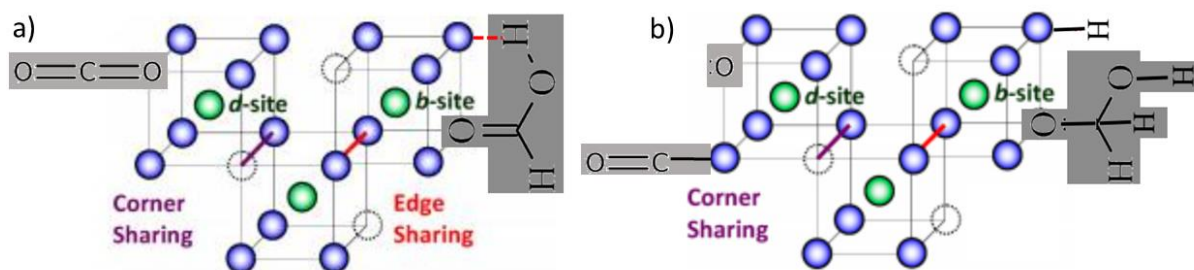


Figure ESI 5: Bixbyite structure of crystalline In_2O_3 with In ions (green), oxide ions (blue) and structural oxide vacancies (open circles) (adapted from Buchholz et al.¹⁴). The grey shaded area shows a suggested binding site for CO_2 before (a) and after (b) shifting a CO group to the neighbouring In, and for formic acid before (a) and after 2-electron-2-proton reduction (b). When the catalyst is prepared with

addition of 0.15 wt% PTFE the indium oxide surface is hydroxylated at reductive potentials, which improves the turnover of HCOOH by a factor of ca. 30. Surface oxygen vacancies were predicted to be important in heterogeneously catalysed hydrogenation of CO₂ on In₂O₃.¹⁵

Tafel plot of formic acid reduction reaction

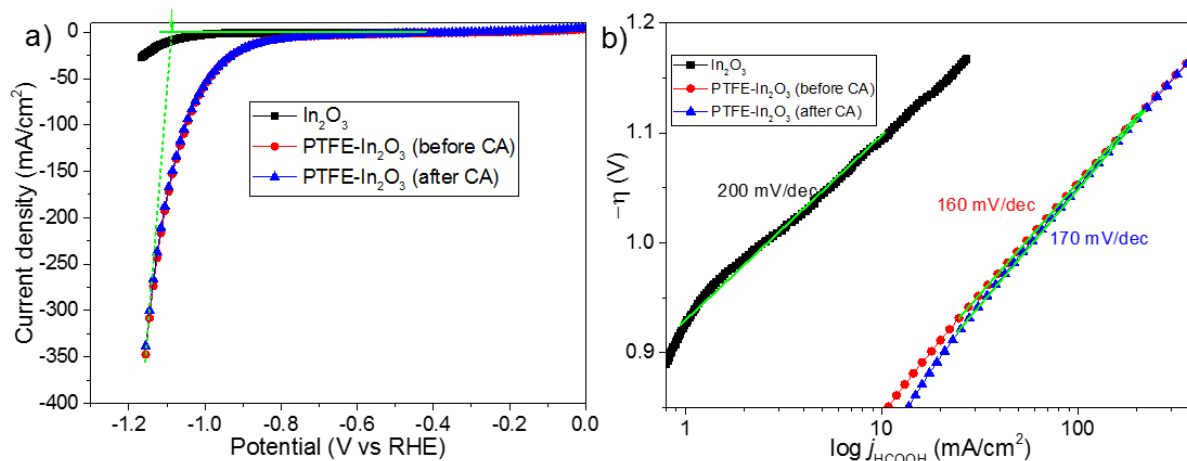


Figure ESI 6: Co-electrolysis of water and aqueous HCOOH (4.3 mol·L⁻¹) conducted with a cell analogous to the one shown in Figure 1a, but with a carbon plate anode and an Ag/AgCl reference electrode. a) Linear sweep voltammetry (sweep rate 10 mV s⁻¹). Black: plain In₂O₃ cathode catalyst (12.5 mg cm⁻², spray-coated on carbon paper); red and blue: In₂O₃ intermixed with 0.30 wt% PTFE before and after a 60 min chronoamperometry (CA) experiment, respectively. The green arrow indicates the onset potential at ca. -1.0 V vs. RHE. The figure demonstrates the greatly enhanced current density when PTFE is added. At the most negative potentials enhanced H₂ formation and the higher catalyst coating contributes to the higher current density in comparison with Figure 4a. b) Tafel plots of LSV curves in a). The slopes reflect the influence of the superposition of the alcohol and H₂ product formation.

PTFE-dependence of product distribution

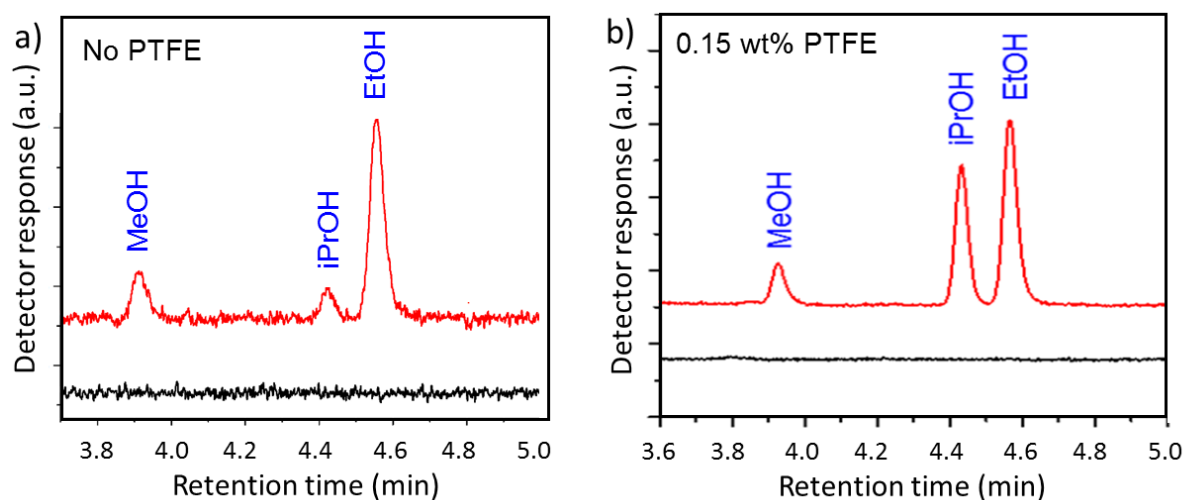


Figure ESI 7: GC analysis of aqueous product phase from co-electrolysis of water and formic acid in the absence (a) and in the presence (b) of 0.15 wt% PTFE in the cathode catalyst. The black trace is before and the red trace after the chronoamperometric experiment at 2.4 V applied cell voltage that leads to product formation. The better signal-to-noise ratio in (b) reflects more efficient product formation. While the relative yields of methanol and ethanol are approximately the same, the yield of iso-propanol is significantly enhanced by the addition of PTFE.

Cell voltage dependence of the energy efficiency

Table S.I. 2: Energy efficiency (%) according to eqn. (2) of main text for co-electrolysis of 4 M formic acid and water as a function of applied cell voltage.

Applied cell voltage / V	Methanol	Ethanol	Iso-propanol	Total
2.0	4.0	14.2	4.4	22.6
2.5	4.6	14.6	4.7	23.9
3.0	4.2	17.9	4.1	26.2
3.5	3.8	16.2	4.2	24.2
4.0	2.5	10.3	2.8	15.6
4.5	1.9	4.9	2.2	9.0
5.0	0.2	0.6	0.4	1.2

References

1. R. Adams and R. L. Shriner, Platinum oxide as a catalyst in the reduction of organic compounds. III. Preparation and properties of the oxide of platinum obtained by the fusion of chloroplatinic acid with sodium nitrate, *J. Amer. Chem. Soc.* 1923, **45**, 2171–2179.
2. C. Felix, T. Maiyalagan, S. Pasupathi, B. Bladergroen and V. Linkov, Synthesis and Optimisation of IrO₂ Electrocatalysts by Adams Fusion Method for Solid Polymer Electrolyte Electrolysers, *Micro and Nanosystems*, 2012, **4**, 186–191.
3. S. Song, H. Zhang, X. Ma, Z. Shao, R. T. Baker and B. Yi, Electrochemical investigation of electrocatalysts for the oxygen evolution reaction in PEM water electrolyzers, *Int. J. Hydrog. Energy*, 2008, **33**, 4955–4961.
4. A. Marshall, B. Børresen, G. Hagen, M. Tsyppkin and R. Tunold, Electrochemical characterisation of Ir_xSn_{1-x}O₂ powders as oxygen evolution electrocatalysts, *Electrochim. Acta*. 2006, **51**, 3161–3167.
5. J. Cheng, H. Zhang, H. Ma, H. Zhong and Y. Zou, Preparation of Ir_{0.4}Ru_{0.6}Mo_xO_y for oxygen evolution by modified Adams' fusion method, *Int. J. Hydrogen Energy*. 2009, **34**, 6609–6613.
6. J. Cheng, H. Zhang, H. Ma, H. Zhong and Y. Zou, Study of carbon-supported IrO₂ and RuO₂ for use in the hydrogen evolution reaction in a solid polymer electrolyte electrolyzer, *Electrochim. Acta*. 2010, **55**, 1855–1861.
7. J. Polonský, I. M. Petrushina, E. Christensen, K. Bouzek, C. B. Prag, J. E. T. Andersen, N. J. Bjerrum, Tantalum carbide as a novel support material for anode electrocatalysts in polymer electrolyte membrane water electrolyzers, *Int. J. Hydrog. Energy*. 2012, **37**, 2173–2181.
8. J. Chandradass, D. S. Bae and K. H. Kim A simple method to prepare indium oxide nanoparticles: Structural, microstructural and magnetic properties, *Adv. Powder Technol.* 2011, **22**, 370–374.
9. O. Martin, A. J. Martin, C. Mondelli, S. Mitchell, T. F. Segawa, R. Hauert, C. Drouilly, D. Curulla-Ferre and J. Perez-Ramirez, Indium Oxide as a superior catalyst for methanol synthesis by CO₂ Hydrogenation *Angew. Chem. Int. Ed.*, 2016, **55**, 6261–6265.
10. J. Polonský, P. Mazúr, M. Paidar, E. Christensen and K. Bouzek, Performance of a PEM water electrolyser using a TaC-supported iridium oxide electrocatalyst, *Int. J. Hydrog. Energy*. 2014, **39**, 3072–3078.
11. L. Sun, R. Ran, G. Wang and Z. Shao, Fabrication and performance test of a catalyst-coated membrane from direct spray deposition, *Solid State Ionics*, 2008, **179**, 960–965.

12. C. Kim, T. Möller, J. Schmidt, A. Thomas, P. Strasser, Suppression of Competing Reaction Channels by Pb Adatom Decoration of Catalytically Active Cu Surfaces During CO₂ Electroreduction. *ACS Catal.*, 2019, **9**, 1482–1488.
13. W. Koutek, A. Conradi, Ch. Fabjan, G. Bauer, In situ FTIR spectroscopy of the Zn – Br battery bromine storage complex at glassy carbon electrode, *Electrochim. Acta*, 2001, **47**, 815–823.
14. D. B. Buchholz, Q. Ma, D. Alducin, A. Ponce, M. Jose-Jacaman, R. Khanal, J. E. Medvedeva and R. P. H. Chang, The structure and properties of amorphous indium oxide. *Chem. Mater.*, 2014, **26**, 5401–5411.
15. J. Ye, C. Liu, D. Mei, Q. Ge, Active oxygen vacancy site for methanol synthesis from CO₂ hydrogenation on In₂O₃(110): a DFT study. *ACS Catal.* 2013, **3** 1296–1306.